



An approach to a multi-walled carbon nanotube based mass sensor

Ramona Mateiu^{a,*}, Zachary J. Davis^a, Dorte N. Madsen^a, Kristian Mølhave^a, Peter Bøggild^a, Anne-Marie Rassmusen^b, Michael Brorson^b, Claus J.H. Jacobsen^b, Anja Boisen^a

^a Department of Micro and Nanotechnology, Danish Technical University (DTU), DK-2800 Kongens Lyngby, Denmark

^b Haldor Topsøe AIS, Nymøllevvej 55, DK-2800 Kongens Lyngby, Denmark

Available online 19 March 2004

Abstract

We propose an approach to a nanoscale mass sensor based on a gold electrode structure, on which a multi-walled carbon nanotube (MWCNT) bridge can be placed and soldered. The structure is comprised of three electrodes with a width of 2 or 4 μm . Two outer electrodes with a length of 10 or 15 μm serve as source and drain electrodes for the MWCNT bridge, whereas an inner electrode with a length of 8 or 13 μm is for electrostatic excitation of the CNT. Some structures have an extra pair of outer electrodes, which may deflect the inner electrodes and thereby be used for stretching or compressing the bridging nanotube. The free standing MWCNTs were fabricated by chemical vapour deposition of Fe(II) phthalocyanine. A nanomanipulator with an $x-y-z$ translation stage was used for placing the MWCNTs across the source–drain electrodes. The nanotubes were soldered onto the substrate by electron beam induced deposition of an organometallic compound.

© 2004 Elsevier B.V. All rights reserved.

Keywords: Multi-walled carbon nanotubes; Electrode substrate; Mass sensor; Electron beam induced deposition; Nanomanipulation

1. Introduction

There is a continuous need for new technologies leading to smaller, faster, more sensitive and cheaper devices. Cantilever based mass sensors are following the same trend. The detection principle in a cantilever based mass sensor is based on the fact that the resonant frequency of the cantilever

depends on the inverse of the square root of the cantilever mass

$$f_{\text{res}} = 0.324 \sqrt{\frac{k}{m_{\text{cantilever}}}}, \quad (1)$$

where f_{res} is the resonant frequency of a rectangular cantilever with a square cross-section, and k is the spring constant of the cantilever. Therefore, a change in the mass of the resonator is detected as a shift in the resonant frequency. By decreasing the dimensions of the resonator, the sensitivity

* Corresponding author. Tel.: +45-4525-5741; fax: +45-4588-7762.

E-mail address: ram@mic.dtu.dk (R. Mateiu).

and spatial resolution of the device are increased. Sensitivities down to 10^{-16} g/Hz [1] have recently been reported for poly-Si cantilever mass sensors. The small dimensions of carbon nanotubes (CNTs) and their extraordinary mechanical properties (tensile strength of ~ 200 GPa [2], Young's modulus ~ 1 TPa [3]) make these structures potential candidates for replacing the vibrating cantilever structure in a mass detector. It has been showed that a 22 fg carbon particle reduces the resonant frequency of a single-walled carbon nanotube (SWCNT) by 40%, which corresponds to a sensitivity of 3×10^{-20} g/Hz [4]. In theory, a SWCNT with a diameter of 0.7 nm, length 100 nm, and a Young's modulus of 1.5 TPa would lead to a sensitivity of 10^{-28} g/Hz. Multi-walled carbon nanotubes (MWCNTs) are easier to manipulate, since they are both longer and have larger diameters than SWCNTs. However, the sensitivity for a MWCNT bridge resonator would only be 0.66×10^{-21} g/Hz for a MWCNT with outer diameter 90 nm, inner diameter 70 nm, length 9 μm , Young's modulus 1 TPa, and density 1.4 g/cm^3 .

Here, we present a chip with gold cantilever electrodes for construction of a mass sensor by placing and soldering a MWCNT across the electrodes.

2. Fabrication

2.1. Substrate fabrication

The chip was fabricated using the process sequence shown schematically in Fig. 1.

First, a 5000 Å thick Si_3N_4 layer is grown on both sides of a 340 μm thick (100)Si wafer by plasma enhanced chemical vapour deposition (PECVD), see Fig. 1(b). The chip pattern is then transferred first to the front side (Fig. 1(c)) and then to the back side (Fig. 1(d)) of the wafer by UV lithography and reactive ion etching (RIE). Next, the electrodes are defined by UV lithography, e-beam evaporation of electrode material, 50 Å Cr as adhesion layer and 7500 Å Au, followed by lift-off, Fig. 1(e). Finally, the electrodes are released by wet anisotropic etch (KOH) of the Si

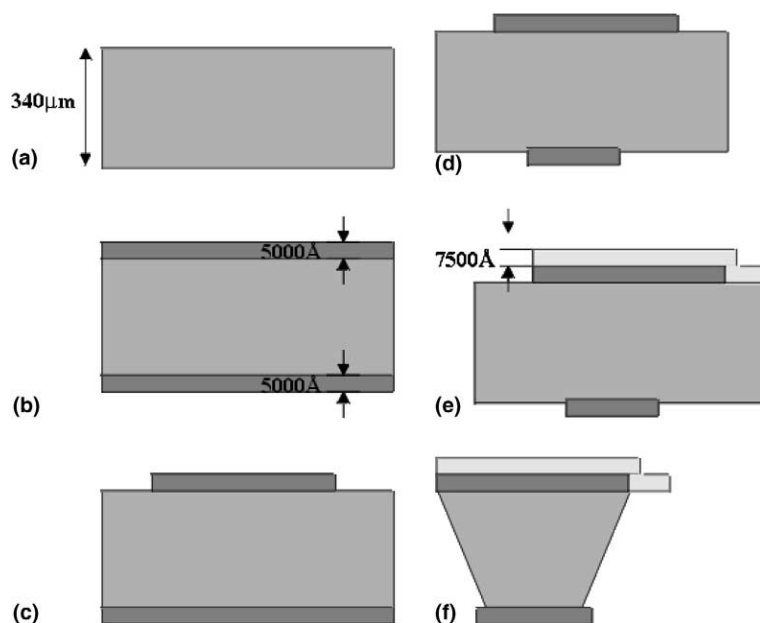


Fig. 1. Schematic drawing of the process sequence for the electrode structure: (a) double side polished silicon wafer; (b) 5000 Å silicon nitride layer grown on both sides of the wafer; (c) and (d) patterning of the front and back side of the chip; (e) electrode patterning by means of gold evaporation; (f) releasing the cantilever by back side anisotropic etch (KOH).

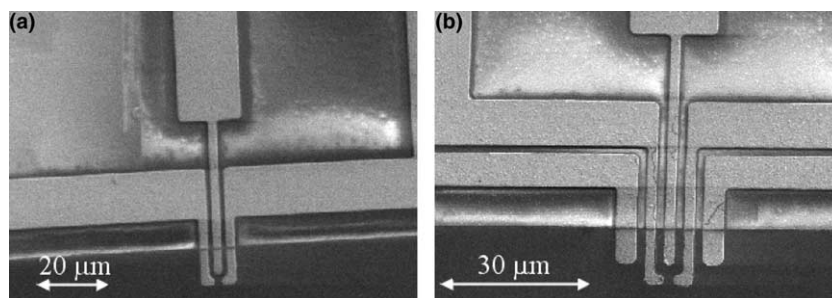


Fig. 2. Scanning electron micrographs of different electrode substrates for positioning of the MWCNT: (a) three electrode chip; (b) five electrode chip, with outer electrodes for electrostatic actuation.

substrate from the back side using a mechanical front side protection (Fig. 1(f)).

Substrates with a various number of differently shaped electrodes (length: 10 or 15 μm , width: 2 or 4 μm) have been realised, see Fig. 2. The MWCNT is soldered on the longer electrodes. The inner electrode is for electrostatic excitation of the tube while the outer thick electrodes can be used to attract the inner electrode pair electrostatically, and thereby stretch the MWCNT. The electrode substrate is glued to a ceramic chip and electrical connections are made by wire bonding.

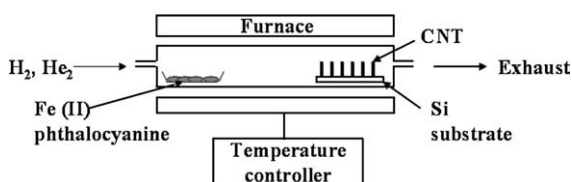


Fig. 3. Schematic drawing of the set-up used for the fabrication of MWCNTs by CVD of Fe(II)phthalocyanine.

2.2. Multi-walled carbon nanotube fabrication

The MWCNTs were fabricated by chemical vapour deposition (CVD) of Fe(II) phthalocyanine, the floating catalyst method [5]. The principle of the method is that the organometallic compound is first evaporated and then decomposed in a flow reactor, see Fig. 3.

A clean quartz boat with a few square pieces, $\sim 2 \text{ cm}^2$, of a Si wafer was placed in the central heated area of the flow reactor. The flow reactor was heated to 950 $^{\circ}\text{C}$ with 10 $^{\circ}\text{C}/\text{min}$. During the heating a H_2 –He flow (1:1, volume ratio, 20 cm^3/min) was maintained. When the flow reactor reached 950 $^{\circ}\text{C}$ a second quartz boat containing 0.9 g Fe(II) phthalocyanine was placed at the entrance. After 5 minutes the H_2 flow was stopped and the flow reactor was cooled down in a He flow. Free standing, nestled, MWCNTs with diameters between 50 and 120 nm, and lengths up to tens of μm were obtained, see Fig. 4(a). A trans-

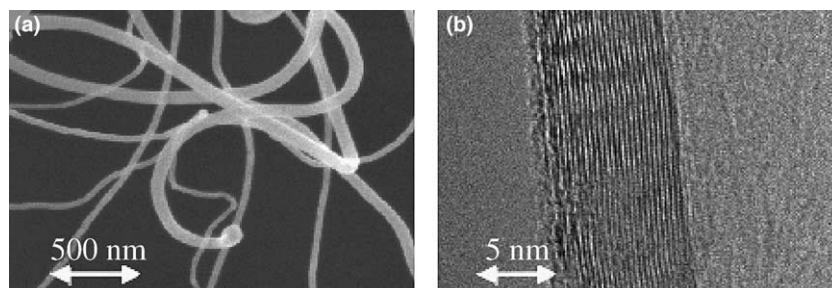


Fig. 4. (a) Scanning electron micrograph of curved MWCNTs. (b) Transmission electron micrograph of one of the MWCNTs. The image shows a cross-section of the shells in one of the side-walls.

mission electron microscope (TEM) analysis shows that the MWCNTs are made of ~ 30 concentric shells, see Fig. 4(b).

3. Results

The manipulation of the MWCNTs onto the electrode substrate was carried out inside an environmental scanning electron microscope (E-SEM), FEI XL 30 E-SEM FEG. The experimental set-up is shown schematically in Fig. 5 and consists of: (i) a Klocke Nanotechnik positioning system with a precision of about 10 nm [6]; (ii) the electrode substrate; (iii) a reservoir for the precursor material, $\text{Me}_2\text{Au}(\text{acetylacetonate})$, used for soldering of MWCNT onto the electrode substrate by electron beam induced deposition (EBID) [7].

The MWCNTs are fixed on a Si substrate and are extending from the edge of the substrate. The electrode structure is approached to the MWCNTs using the nanomanipulator. During the experimental work we discovered that the best manipulation strategy is to approach the electrode substrate from underneath a free standing MWCNT until it touches the CNT, see Figs. 5 and 6(a). This can easily be observed in the SEM due to a change in contrast of the tube. When the CNT is touching the grounded electrode, the tube immediately appears darker in the SEM image. Approaching the tube with the electrode system coming from above proved to be tedious. In this configuration the tubes are difficult to manipulate on top of the electrodes. It is practically impossible to determine whether the tube makes contact with the electrodes merely by looking at the SEM image.

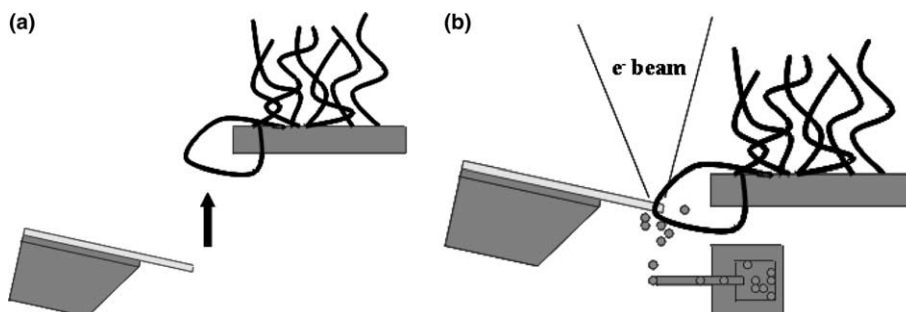


Fig. 5. (a) Schematic of the manipulation experiment. The electrode substrate is approaching from underneath a free standing MWCNT, which lies across the edge of the tubes substrate. (b) Schematic of the soldering experiment. When the MWCNT make contact to the electrode substrate, EBID is used to make the mechanical and electrical connection.

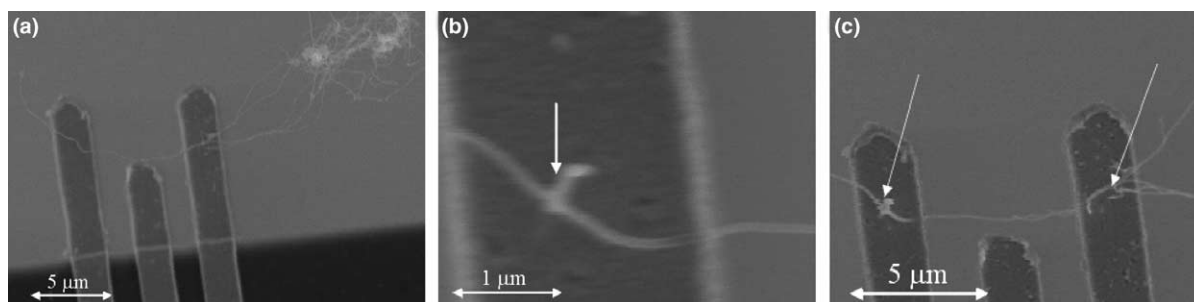


Fig. 6. (a) Electrode based substrate approaching a MWCNT from underneath. (b) MWCNT soldered onto one of the electrodes of the substrate. The arrow indicate the solid deposit from EBID of $\text{Me}_2\text{Au}(\text{acetylacetonate})$. (c) MWCNT soldered at both ends onto the electrodes.

When the CNT is bridging the gap between the longer electrodes, the next step is to mechanically and electrically connect it to the electrodes by means of EBID of an organometallic compound, see Fig. 5(b). In the presence of H₂O vapour, the electron beam induced deposits from Me₂Au(acetylacetonate) turn out to be mechanically strong, and highly conductive [7,8]. By interconnecting two electrodes entirely by the soldering material the conductivity was found to be two orders of magnitude smaller than that of pure bulk gold.

Fig. 6(b) shows a deposit from Me₂Au(acetylacetonate), which is fixing the MWCNT on the left electrode. The MWCNT is soldered onto a cantilever electrode at both ends, see Fig. 6(c). Finally, the substrate with the tube fixed on it is pulled away from the MWCNTs substrate.

4. Conclusion

An electrode substrate, which can be used as a platform for a MWCNT based mass sensor has been produced by Si batch fabrication. MWCNTs were produced by CVD of Fe(II)phthalocyanine and the resulting tubes were free standing and highly curved, with a diameter between 50 and 120 nm, and lengths up to tens of μm . A MWCNT was soldered onto the longer electrodes on the substrate by means of EBID of Me₂Au(acetylacetonate). Further experiments need to be done in order to detect the resonant frequency of the tube. One straightforward mass detection experiment would be to deposit gold onto the MWCNT by EBID, and monitor the changes in the resonant frequency of the tube. The expected mass sensitivity for a mass detector based on one of the MWCNTs produced by CVD of Fe(II) phthalocyanine is ideally 0.66×10^{-21} g/Hz, which is four orders of magnitude higher than the sensitivity of one of the previous cantilever based mass detectors reported [1]. It may however be that the Young's modulus of the nanotube is diminished by the presence of defects, as commonly found in CVD grown nanotubes. The kinks and bends on the nanotubes suggest that there may be a substantial amount of defects, see Fig. 4(a). Experiments with near-perfect, arc-discharge grown carbon nanotubes are planned for the future.

cyanine is ideally 0.66×10^{-21} g/Hz, which is four orders of magnitude higher than the sensitivity of one of the previous cantilever based mass detectors reported [1]. It may however be that the Young's modulus of the nanotube is diminished by the presence of defects, as commonly found in CVD grown nanotubes. The kinks and bends on the nanotubes suggest that there may be a substantial amount of defects, see Fig. 4(a). Experiments with near-perfect, arc-discharge grown carbon nanotubes are planned for the future.

Acknowledgements

We acknowledge Haldor Topsøe A/S for allowing us to perform our manipulation and soldering experiments into their E-SEM.

References

- [1] Z.J. Davis, G. Abadal, E. Forsén, O. Hansen, F. Campabadal, E. Figueras, J. Esteve, J. Verd, F. Perez-Murano, X. Borriase, S.G. Nilsson, I. Maximov, L. Montelius, N. Barniol, A. Boisen, *Int. Conf. Sensor. Actuator., Transducers* (2003) 496–499.
- [2] NASA web page.
- [3] H. Dai, J.H. Hafner, A.G. Rinzler, D.T. Colbert, R.E. Smalley, *Nature* 384 (1996) 147–151.
- [4] Z.L. Wang, P. Poncharal, W.A. de Heer, *J. Phys. Chem. Solids* 61 (2000) 1025–1030.
- [5] X. Wang, Y. Liu, D. Zhu, *Chem. Commun.* (2001) 751–752.
- [6] Klocke Nanotechnik, Documentation: Nanomotor and Positioner, Network Controller, Software.
- [7] D.N. Madsen, K. Mølhave, R. Mateiu, A.M. Rasmussen, M. Brorson, C.J.H. Jacobsen, P. Bøggild, *NanoLetters* 3 (2003) 47.
- [8] K. Mølhave, D.N. Madsen, A.M. Rasmussen, A. Carlsson, C.C. Appel, M. Brorson, C.J.H. Jacobsen, P. Bøggild, *NanoLetters* 3 (2003) 1499.